Stepwise Charge Separation from a Ruthenium−Tyrosine Complex to a Nanocrystalline TiO_2 Film

Jingxi Pan,[†] Yunhua Xu,[‡] Gabor Benkö,[†] Yashar Feyziyev,[§] Stenbjörn Styring,[§,||] Licheng Sun,[‡] Björn Åkermark,[‡] Tomáš Polívka,[†] and Villy Sundström*,[†]

Department of Chemical Physics, Lund University, Box 124, S-22100 Lund, Sweden, Department of Organic Chemistry, Stockholm University, S-10691 Stockholm, Sweden, Department of Biochemistry, Lund University, Box 124, S-22100 Lund, Sweden, and Molecular Biomimetics, Uppsala University, Villavagen 6, S-75236 Uppsala, Sweden

Received: February 6, 2004; In Final Form: May 4, 2004

A supramolecular complex composed of Ru(II) tris-bipyridine, tyrosine, and dipicolylamine was synthesized and characterized. This complex was attached to TiO_2 nanocrystalline films via ester groups at the Ru(II) chromophore, and photoinduced multistep electron transfer was investigated by laser flash photolysis and electron paramagnetic resonance techniques. Following ultrafast electron injection from the metal−ligand charge transfer excited states of Ru(II) to the conduction band of TiO_2, fast intramolecular electron transfer from the tyrosine moiety to the photogenerated Ru(III) was observed, characterized by a rate constant of $\sim 2 \times 10^6$ s^{-1}. By comparison of recovery kinetics at the isosbestic point with that of the reference compound lacking the tyrosine, it was found that the intramolecular electron-transfer efficiency is 90%. A hydrogen-bond-promoted electron-transfer mechanism is proposed.

1. Introduction

Among the dye-sensitized nanocrystalline solar cells, a classical example is the "Grätzel" solar cell, developed by Grätzel and co-workers in 1991 using a Ru-bipyridyl-based sensitizer, for which a light-to-electricity conversion yield of ~10% was achieved.[1] A working cycle of such a solar cell starts with excitation of a dye bound to the TiO_2 film, enabling an ultrafast electron injection (EI) from excited states of the dye into the conduction band of the TiO_2 semiconductor ($S^*|TiO_2 \rightarrow S^+|(e_{cb}^-)TiO_2$). The oxidized dye ($S^+$) is then reduced to the parent molecule by a reversible redox mediator (typically iodide). Due to their cheap fabrication together with other attractive features, these solar cells have attracted considerable interest in recent years,[2] and the efforts were mostly focused on improving the conversion efficiency. One of the many strategies to improve the efficiency is to prevent direct charge recombination between oxidized dye and electrons in the conduction band of TiO_2 and, consequently, to prolong the lifetime of the charge-separated state.[3] Such a situation can be achieved by removing the positive hole (generated after EI from the metal−ligand charge transfer (MLCT) state of the dye to the semiconductor) away from the surface of the semiconductor film.

To fulfill this strategy, several studies have been carried out to directly place the redox active chromophore unit away from the TiO_2 surface.[4−6] Dye sensitizers with organic spacers that increase the distance between the binding groups and the chromophore were prepared, slowing down the recombination rate substantially.[4,5] A drawback of this approach, however, is a slower EI rate[4] that could decrease the total injection efficiency. Another approach involved a construction of binuclear Ru(II)−Rh(III) complexes that can fulfill stepwise electron injection (from Ru(II) to Rh(III) and then to TiO_2).[6] However, in this case, the efficiency for the second step was only 40% because of competing primary charge recombination. Furthermore, in some cases, the lifetime of the charge-separated states was shorter than that of a similar compound without the spacer.[5]

In comparison with these two alternatives, introducing an additional electron donor into the dye molecule might be a more feasible way because we can choose an electron donor that can efficiently reduce the photo-oxidized dye molecule but does not affect the EI process. In principle, this should be possible since it has been demonstrated that the EI process occurs on an ultrafast time scale (femtoseconds−pisoseconds)[7−9] in dye-sensitized solar cells, while the back electron transfer occurs on a much slower time scale, up to miliseconds.[4,9,10] Several molecular dyads with artificial electron donors have been studied for this purpose, but the success has been limited.[3,8,11,12] When the electron donor was Os(II), no significant photocurrent was observed because the iodide oxidation by Os(III) could not compete kinetically with primary charge recombination due to its too low redox potential.[11] On the other hand, if the one-electron oxidation potential of the electron donor is higher than that of the sensitizer,[8] it will be a very inefficient donor. Also, the distance between the electron donor and the chromophoric unit in a dyad is an important factor, which may influence the quenching of dye excited states and affect the EI efficiency.[3] In addition, it was recently shown that introducing a triarylamine subunit into ruthenium terpyridine complexes did not increase their photovoltaic performances. This was attributed mainly to an additional short-circuiting pathway in the photoanode incorporating these dyads.[3]

To reduce the recombination rate on the dye−semiconductor interface, we make use of charge-stabilizing processes occurring in photosystem II of natural photosynthesis. Here a tyrosine side

* To whom correspondence may be addressed. Fax: +46-46-222 4119. E-mail: villy.sundstrom@chemphys.lu.se.
[†] Department of Chemical Physics, Lund University.
[‡] Stockholm University.
[§] Department of Biochemistry, Lund University.
[||] Uppsala University.

10.1021/jp049449v CCC: $27.50
Published on Web 08/04/2004

CHART 1: Molecular Structure of RuTP and the Reference Compound RuAla

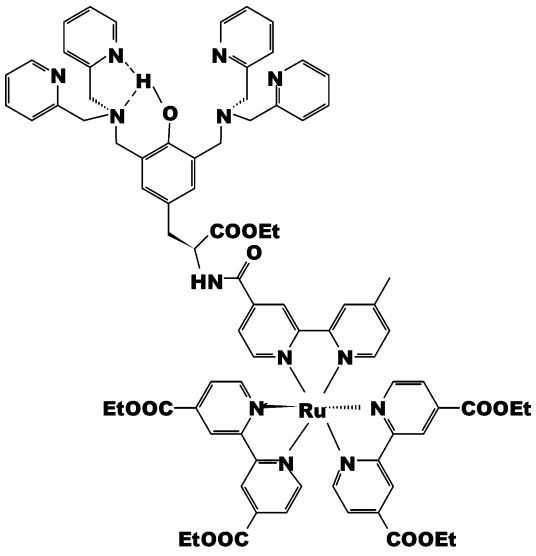

chain has evolved as the immediate electron donor to the oxidized primary donor P_{680}^+, and charge-separation efficiency close to unity is achieved.[13] To mimic this function of nature, we have synthesized a ruthenium(II)−tris-bipyridine complex (which mimics P_{680}) coupled with tyrosine. The complex was anchored to the surface of TiO_2 nanoparticles via carboxylic acid groups.[14] However, the intramolecular electron transfer (ET) efficiency obtained for this system was only 15%. In recent years, strong evidence has been presented for hydrogen bonding between the tyrosine in PS II and a nearby base, most likely a histidine residue (D1−His_{190}).[15] This hydrogen bond may play a crucial role in the efficient electron-transfer reaction. A supramolecular complex containing dipicolylamine (dpa) ligands, which mimics His_{190}, was therefore designed and synthesized.[16] In the present study, we report on time-resolved spectroscopy and electron paramagnetic resonance (EPR) studies of a related complex (RuTP, Chart 1) containing ester groups for attachment to nanocrystalline TiO_2 film. Additionally, a complex containing alanine (RuAla, Chart 1) instead of tyrosine was used as a reference.

2. Experimental Section

Materials. Acetonitrile (99.5+%) and lithium perchlorate (99+%) were obtained from Merck and Fluka, respectively, and used as received. TiO_2 paste (average particle size ∼13 nm in colloidal solution) was purchased from Solaronix SA. All other chemicals were purchased from Aldrich or Lancaster and used as received. All solvents were dried by standard methods. Silica gel 60 (0.043−0.063 mm, Merck, Darmstadt, Germany) was used for column chromatography. *cis*-Ru(4,4′-di-COOEt-2,2′-bpy)$_2$Cl$_2$ (**1**),[14] 4′-methyl-2,2′-bipyridine-4-carboxylic acid (**2**),[17] NH_2−CH(COOEt)-HBPMP (**4**),[16] and the reference complex (RuAla)[14] were prepared according to the literature methods.

[Ru(4,4′-di-COOEt-2,2′-bpy)$_2$(4-Me-4′-COOH-2,2′-bpy)](PF$_6$)$_2$ (3). A mixture of *cis*-Ru(4,4′-di-COOEt-2,2′-bpy)$_2$Cl$_2$ (**1**) (433 mg, 0.56 mmol) and silver triflate (288 mg, 1.12 mmol) in acetone (20 mL) was stirred for 10 h at room temperature under nitrogen. The solution turned gradually orange, and a white precipitate of AgCl was formed. AgCl was removed by filtration, and 4′-methyl-2,2′-bipyridine-4-carboxylic acid (**2**) was added to the filtrate. The reaction mixture was refluxed for 8 h under nitrogen. Water (15 mL) was added to the mixture, and acetone was removed by rotary evaporation. Then a saturated aqueous solution of NH_4PF_6 was added to the mixture until no further precipitate was observed. The solid was collected by filtration, washed with water and ether, and dried in a vacuum. Purification was made by a column on silica gel using MeCN/H_2O/KNO_3 (saturated) (20/3/1) as eluent. After column, the solvent was evaporated, and the solid dissolved in a minimum amount of water. Reprecipitation by addition of saturated NH_4PF_6 gave 370 mg (55%) of the desired product. ^{1}H NMR (400 MHz, CD_3CN), δ in ppm: 1.40−1.46 (t+t, J = 7.2 Hz, 12H, −COOCH_2CH_3); 2.58 (s, 3H, bpy′-CH_3); 4.44−4.52 (q+q, J = 7.2 Hz, 8H, −COOCH_2CH$_3$); 7.31 (d, J = 5.2 Hz, 1H, bpy′−*H*); 7.51 (d, J = 6.0 Hz, 1H, bpy′−*H*); 7.78−7.95 (m, 10H, bpy−*H*+bpy′-*H*); 8.59 (s, 1H, bpy′−*H*); 8.93 (s, 1H, bpy′-*H*); 9.07 (s, 4H, bpy−*H*).

[Ru(4,4′-di-COOEt-2,2′-bpy)$_2$-4-Me-4′-CONH−CH(COOEt)-HBPMP](PF$_6$)$_2$ (RuTP). 3 (470 mg, 0.39 mmol) was refluxed in 15 mL of $SOCl_2$ for 3 h. Excess of $SOCl_2$ was removed under reduced pressure, and the residue was dried under vacuum at 50 °C for 1 h. The resulting solid (acid chloride) was redissolved in 5 mL of dry CH_2Cl_2. The solution was added dropwise to a solution of **4** (265 mg, 0.42 mmol) and triethylamine (0.5 mL) in dry CH_2Cl_2 (10 mL). The resulting solution was stirred under argon at room temperature overnight. The solvent was removed, and water (50 mL) was added. Then it was extracted with CH_2Cl_2 (4 × 50 mL). The crude product was purified on a column of silica gel using a mixture of MeCN/H_2O/KNO_3 (saturated) (40/3/1) as eluent. After column, the solvent was evaporated, and the solid was dissolved in a minimum amount of water, and saturated aqueous solution of NH_4PF_6 was added. The mixture was extracted with CH_2Cl_2, and the combined organic phase was washed with a diluted Na_2CO_3 aqueous solution and then dried over Na_2SO_4. Solvent was removed under reduced pressure to afford 450 mg (63%) of the desired product. ^{1}H NMR (400 MHz, acetone-d_6), δ in ppm: 1.17 (t, J = 6.8 Hz, 3H, Tyr-CO$_2$CH$_2$CH_3); 1.3−1.4 (m, 12H, bpy-CO$_2$CH$_2$CH_3); 2.57 (s, 3H, bpy′-CH_3); 3.00−3.20 (m, 2H, Ph−CH_2−CH(CO$_2$Et)−); 4.14 (q, J = 7.2 Hz, 2H, Tyr-CO$_2$CH_2CH$_3$); 4.20−4.28 (m, 12H, N(CH_2−)$_3$); 4.34−4.50 (m, 8H, bpy-CO$_2$CH_2CH$_3$); 4.80−4.88 (m, 1H, −C*H*(CO$_2$Et)−); 7.25 (s, 2H, Ph−*H*); 7.41−7.49 (m, 10H, Py−*H* (8H) + bpy′−*H* (1H) + −CON*H*−); 7.79−8.00 (m, 10H, Py−*H* (4H) + bpy−*H* (4H) + bpy′−*H* (2H)); 8.18−8.40 (m, 5H, bpy−*H* (4H) + bpy′−*H* (1H)); 8.60−8.70 (m, 5H, Py−*H*+ bpy′−*H*); 8.95−8.99 (m, 1H, bpy′−*H*); 9.25−9.30 (m, 4H, bpy−*H*), 11.05 (s, 1H, Tyr-O*H*). ESI-MS (*m*/*z*): 1820.5 (calcd. for [M + H$^+$], 1820.5); 837.7 (calcd. for [M + H$^+$−PF$_6^-$]$^{2+}$, 837.7).

TiO$_2$ Film Preparations. To obtain a nanocrystalline TiO_2 film of uniform thickness, we used scotch tape as a framer and a glass rod to spread a drop of viscous TiO_2 suspension onto a

$76 \times 26 \times 1$ mm^3 microscope glass slip. After removing the tape and drying in air at room temperature for about 2 h, it was sintered at 420−440 °C for 30 min to form a transparent TiO_2 film. The thickness of the film was measured to be about 6 μm by both interference pattern in the steady-state absorption spectrum and a profilometer.

Dye sensitization of the TiO_2 film was carried out by soaking the still hot (80 °C) film in a ~5 mM acetonitrile (CH_3CN) solution of the dye and incubated at room temperature for about 24 h. After the sensitization procedure, the film was rinsed with acetonitrile to wash off the nonattached dye, dried at room temperature, covered with acetonitrile containing $LiClO_4$ (0.1 M) and another microscope glass slip, and finally sealed. $LiClO_4$ was used because it has been shown that lithium cations can increase electron injection quantum yield with no discernible influence on the rate of charge recombination.[10c] Surface-bound RuAla and RuTP are further referred to as RuAla−TiO_2 and RuTP−TiO_2, respectively. Steady-state absorption spectra of the dye-sensitized TiO_2 films were recorded before and after the flash photolysis experiments to ensure that no dye degradation occurred during time-resolved measurements. All the dye-sensitized films were freshly prepared and kept in the dark before all measurements.

Spectroscopy. Steady-state absorption measurements were carried out on a Jasco-V-530 spectrophotometer. Photoluminescence spectra were recorded using a Spex Flurolog fluorimeter by exciting the sample at 450 nm. Transient absorption and emission measurements were carried out using a nanosecond laser flash photolysis setup described elsewhere.[18] Briefly, excitation pulses at 450 nm (0.4 mJ, 7 ns full width at half maximum) were obtained from a Quanta-Ray master optical parametric oscillator (MOPO) pumped by a Quanta-Ray 230 Nd:YAG laser (355 nm). The probe light was provided by a 75-W Xe arc lamp and was collinear with the excitation beam. After passing through the sample, the probe light was spectrally filtered using two monochromators and finally detected by a Hamamatsu R928 photomultiplier tube. To prevent degradation of the dye due to laser light irradiation, samples in solution were measured in a 1-cm quartz cell with stirring by a magnetic stirrer, and samples on TiO_2 film were kept moving during measurements by using a $X-Y$ translation stage. Individual trace kinetics were analyzed using the deconvolution software Spectra Solve 2.01, Lastek Pty. Ltd. (1997).

EPR studies were performed with a Bruker E580 ELEXSYS spectrometer using a ST4102 resonator (Bruker Analytic, Gmb H, Karlsruhe, Germany). EPR setting parameters are shown in the figure legends. Experiments with continuous light illumination of the EPR sample were performed at room temperature with white light from an 800-W projector lamp. The white light was filtered through a 5 cm thick $CuSO_4$-water (3%) solution and directed into the cavity using a Perspex light guide.

3. Results and Discussion

Synthesis. Synthesis of the reference complex RuAla was described previously.[14] The RuTP complex was prepared in a similar procedure to that for the analogue without four ester groups in the bipyridines (Scheme 1).[16] The ruthenium(II)−trisbipyridine complex **3** was prepared from dichloro ruthenium-(II) bis(4,4′-di-COOEt-bipyridine) (**1**)[14] and 4′-Me-4-COOH-bipyridine (**2**).[17] It was first chlorinated with $SOCl_2$, then coupled with NH_2−CH(COOEt)−HBPMP (**4**)[16] followed by purification on column, to afford the desired complex RuTP. All complexes were characterized by ^{1}H NMR and ESI-MS. The ^{1}H NMR signal of the phenolic proton in complex RuTP appears at 11 ppm, indicating a strong hydrogen-bonding in the complex.

SCHEME 1: Synthetic Routes for the Complex RuTP

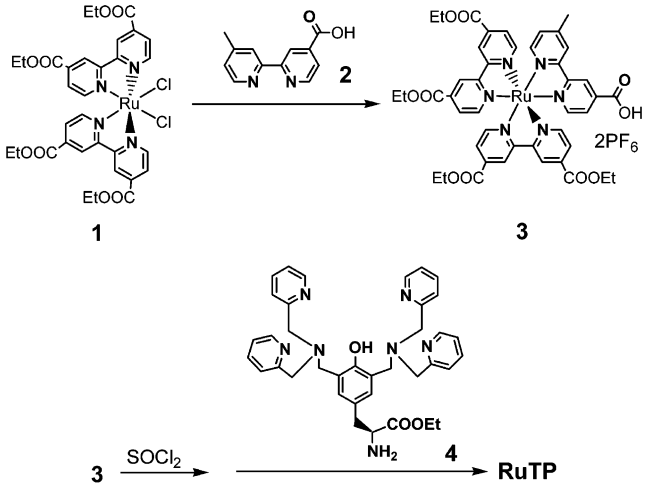

Steady-State Measurements. Figure 1 shows the steady-state absorption and emission spectra of RuTP. The shape and position of the main absorption band on TiO_2 film are very similar to that of RuTP in acetonitrile, and both exhibit the MLCT band centered at 470 nm, characteristic of ruthenium trisbipyridine complexes.[19] The increase of absorbance below 400 nm when attached to the TiO_2 film is mainly due to the absorption of TiO_2 and light scattering. Thus, it is concluded that the surface attachment has no significant effect on the photophysical properties of RuTP. This result is not surprising, as the electronic coupling of the ethyl carboxylate group to TiO_2 is less than that of the carboxyl group (for which broadening and red-shift of the absorption spectra is usually observed).[4,9,20] This conclusion is further supported by the fact that the emission spectrum of RuTP−TiO_2 is nearly identical to that of RuTP in solution (Figure 1). However, under condition of identical optical densities of RuTP on the film and in solution, the intensity of the emission is much lower for RuTP−TiO_2, indicating considerable quenching of the excited state by electron injection into TiO_2 (further evidence is provided in the transient absorption measurements). Similar results were obtained for the RuAla reference compound (data not shown), demonstrating that the tyrosine part has almost no effect on the photophysical properties of the complex. In addition, the emission decays of RuTP (Figure 2) and RuAla (data not shown) in acetonitrile solution follow single exponential kinetics with time constants of 1150

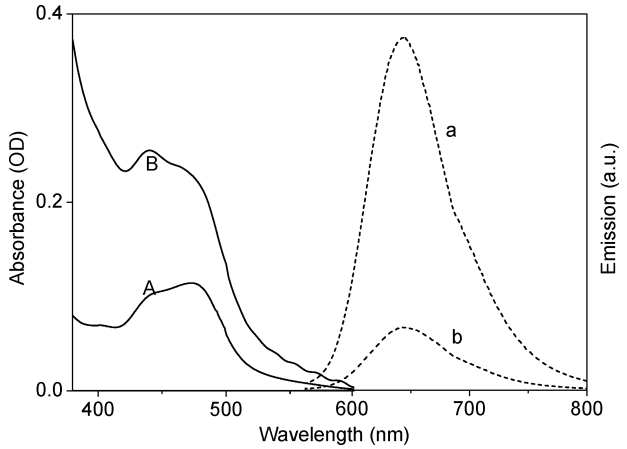

Figure 1. The steady-state absorption and photoluminescence spectra of RuTP. (A) absorption and (a) photoluminescence in acetonitrile containing 0.1 M $LiClO_4$; (B) absorption and (b) photoluminescence on TiO_2 film.

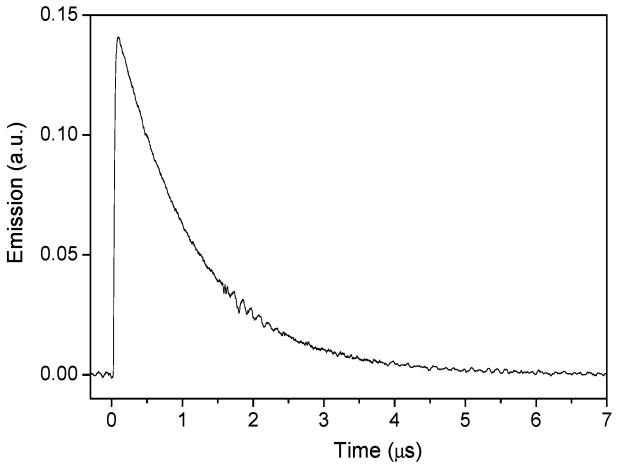

Figure 2. Emission kinetics of RuTP at 640 nm in acetonitrile.

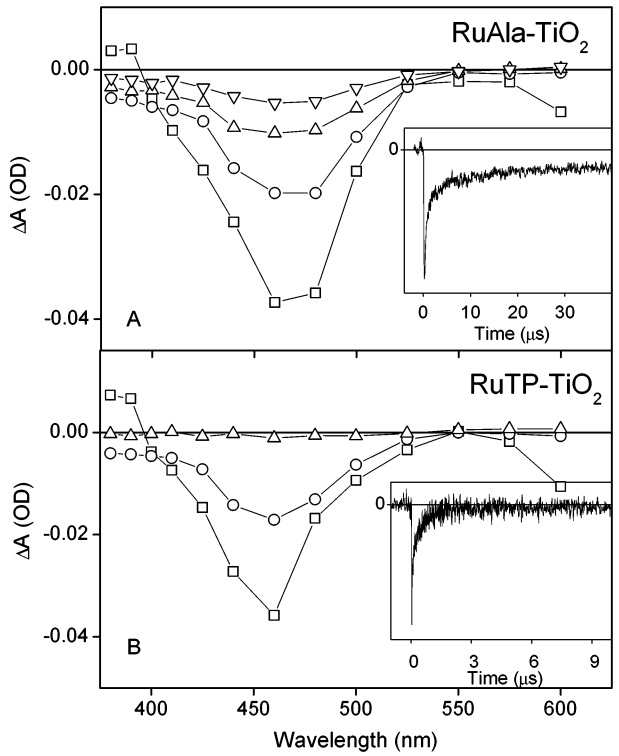

Figure 3. The time-resolved absorption difference spectra recorded after pulsed light excitation at 450 nm of the dye-sensitized films in 0.1 M $LiClO_4$ acetonitrile. For RuAla−TiO_2 (A), the data were recorded at 50 ns (□), 500 ns (○), 2 μs (△), and 20 μs (▽). For RuTP−TiO_2 (B), the data were recorded at 50 ns (□), 200 ns (○), and 2 μs (△). The insets display the recovery kinetics at 470 nm.

and 1120 ns, respectively. Thus, the tyrosine moiety does not quench the excited states of the ruthenium chromophore and consequently will not affect the electron injection process. A comparable lifetime of 1350 ns was obtained for a ruthenium−tyrosine complex similar to RuTP,[16] in which the bipyridine ligands lack the ethyl carboxylate group.

Time-Resolved Absorption Studies. The transient absorption spectra obtained after 450-nm excitation of RuAla−TiO_2 and RuTP−TiO_2 are shown in Figure 3. At 50 ns delay, the transient spectra of both complexes are dominated by a strong bleaching band centered at around 460 nm, together with a weak positive absorption at 390 nm and an emission band above 550 nm. The last two features are ascribed to a signal originating from the triplet MLCT state of Ru(II), since it decays on the sub-100-ns

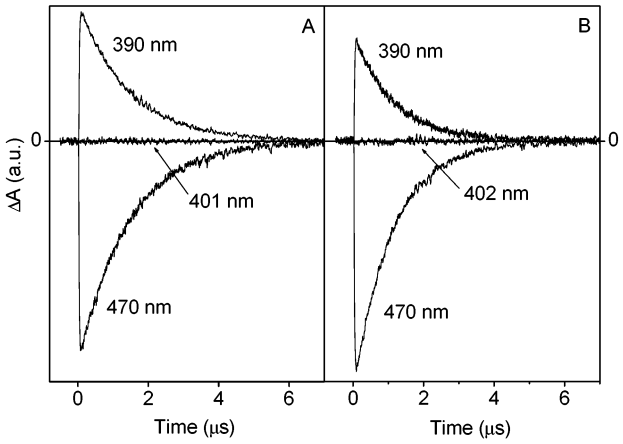

Figure 4. Transient absorption kinetics at selected wavelengths of RuAla (A) and RuTP (B) in deoxygenated acetonitrile containing 0.1 M $LiClO_4$.

time scale and resembles well the features observed in an early-time transient spectrum of the complexes in solution (data not shown). The presence of Ru(II) excited states in the 50-ns transient spectrum signals that a fraction of the attached complexes exhibits less efficient or even no injection, which is also obvious from the emission spectra as the attachment does not quench emission completely (Figure 1). Consequently, the EI efficiency in this system is not 100%, even in the presence of 0.1 M lithium cations, which is consistent with a recent report on a similar ruthenium dye with the same binding group.[10c] Following the decay of the Ru(II) triplet MLCT state, the transient absorption spectra show mainly the bleaching of the Ru(II) chromophore as a result of formation of Ru(III), which is created as a product of electron injection from the MLCT state to the conduction band of TiO_2.[6,7,10c,14] Since the extinction coefficients of both Ru(III) trisbipyridine and the electrons in the conduction band are much smaller than that of Ru(II) trisbipyridine in our spectral window,[19a,20] the bleaching of Ru(II) chromophores dominates at longer delays and no new absorption features attributable to the oxidized dye or injected electrons are observed.

Although the spectral profile of the Ru(II) bleaching is very similar for both RuAla−TiO_2 and RuTP−TiO_2 complexes, their time evolution is dramatically different. For RuAla−TiO_2, the bleaching signal exhibits a multiexponential decay (see below) and a signal of a substantial magnitude is still observed at 20 μs (Figure 3A). In the case of RuTP−TiO_2, however, the bleaching signal decays almost completely within the first 2 μs, which indicates that Ru(III) generated by electron injection is quickly reduced by an electron coming from the attached tyrosine-dpa moiety, and this intramolecular ET successfully competes with the back charge recombination.

To obtain information about the efficiency of the intramolecular ET, it is necessary to perform a detailed analysis of the kinetics of bleaching recovery of the Ru(II). The kinetics recorded at the bleaching maximum of 470 nm (Figure 3B inset) proves the presence of intramolecular ET, but since the initial part of the decay represents a mixture of processes originating from both electron injection and the decay of MLCT excited states, it is not possible to use these kinetics to calculate the yield of intramolecular ET. However, on the basis of the transient absorption kinetics in deoxygenated acetonitrile solution (Figure 4), the isosbestic points for RuAla and RuTP are found to be located at 401 and 402 nm, respectively. Therefore, the kinetics recorded for RuAla−TiO_2 and RuTP−TiO_2 at these

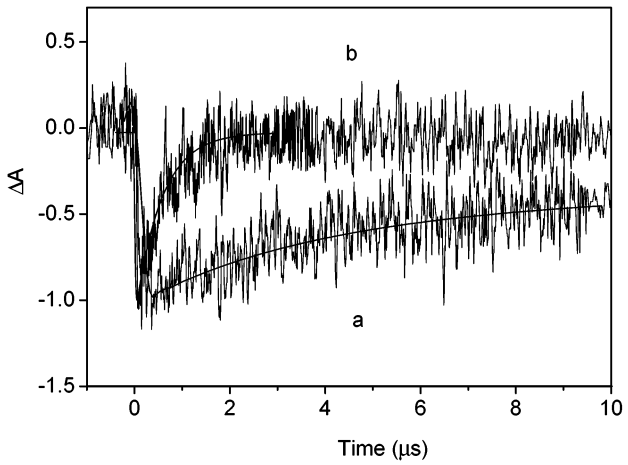

Figure 5. Kinetic traces at 401 nm of RuAla−TiO_2 (a) and 402 nm of RuTP−TiO_2 (b) after 450 nm light excitation and overlaid kinetic fits: (a) 3.6 μs (47%), 24 μs (23%), 212 μs (24%), >1 ms (6%); (b) 550 ns.

wavelengths are free from contributions of excited states. For RuAla−TiO_2, the trace at 401 nm (Figure 5, trace a) represents the kinetics of charge recombination of Ru(III) with the electrons in the conduction band. To obtain a satisfying fit, at least four time constants ($\tau_1 = 3.6\ \mu$s (47%), $\tau_2 = 24\ \mu$s (23%), $\tau_3 = 212\ \mu$s (24%), $\tau_4 > 1$ ms (6%)) are necessary, demonstrating a multiexponential nature of the charge recombination process, which is typical for dye−TiO_2 systems.[4,6,10] For RuTP−TiO_2, the kinetics at the isosbestic point is much faster (Figure 5, trace b). Since there is no contribution from the excited states, it represents the recovery of Ru(II) caused by intramolecular ET. It is fitted well with a single-exponential decay characterized by a time constant of 0.55 μs. Assuming that the increase of recovery rate in the RuTP−TiO_2 system is caused entirely by intramolecular ET, the quantum yield (Φ_{et}) of intramolecular ET from the tyrosine-dpa moiety to Ru(III) can be estimated from the following equation

$$\Phi_{et} = \sum_{n=1}^{4} (1 - \tau_0/\tau_n)\phi_n$$

where τ_0 is the decay time at the isosbestic point for RuTP−TiO_2 system, τ_n are the individual decay time constants at the isosbestic point for RuAla−TiO_2, and ϕ_n are relative amplitudes of the τ_n decay components. Using this equation leads to the yield of $\Phi_{et} = 0.92$, which means that most of the positive holes produced after electron injection were transferred to the tyrosine-dpa moiety. Considering that there are four ester groups on the bipyridine ligands, several different binding modes between RuTP and TiO_2 are expected, and this may result in different distances between the tyrosine-dpa moiety and the TiO_2 surface. However on the average, after intramolecular ET, the distance between the positive holes and the electrons in the conduction band of TiO_2 should be much longer than that in the RuAla−TiO_2 reference system.

In previous studies on dyads containing Ru(II) trisbipyridine and tyrosine derivatives, it has been shown that tyrosine can act as an effective electron donor for Ru(III) reduction both in solution in the presence of an external electron acceptor,[16,21,22] and on TiO_2 in colloidal solution.[14] The use of an external electron acceptor such as MV^{2+} would make the analysis of spectral features rather complicated, since the absorption of $MV^{\bullet+}$ overlaps with that of the tyrosyl radical (390−410 nm),[23] which is generated as a result of intramolecular ET.[21,22] In

SCHEME 2: Reaction Mechanism Proposed for the Photoinduced Electron Transfer in the RuTP−TiO_2 System[a]

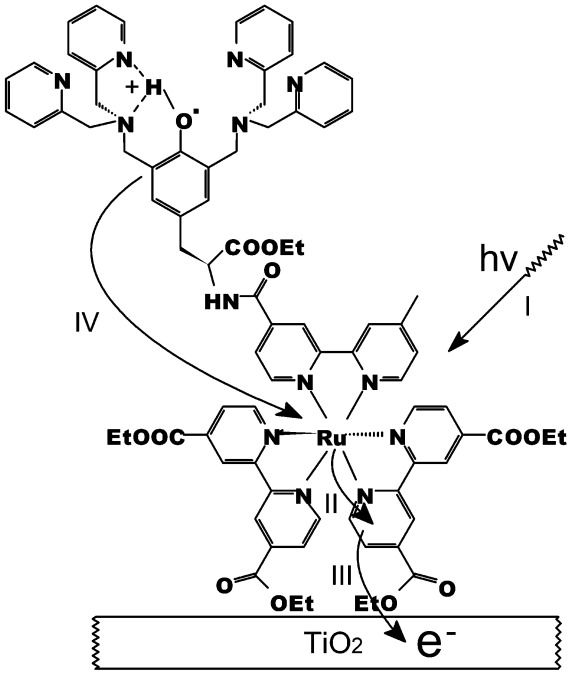

[a] Key: (I) Light excitation; (II) MLCT; (III) electron injection from the MLCT excited state to the conduction band of TiO_2; (IV) intramolecular ET from the hydrogen-bonded tyrosine moiety to Ru(III) with 90% efficiency leading to tyrosyl radical formation.

contrast, using TiO_2 should make it possible to monitor the tyrosyl radical directly, because the spectral region of interest is free from other contributions.[14] Here, however, as it is obvious from the transient spectra shown in Figure 3B, no spectral features attributable to the tyrosyl radical were detected. There are two possibilities for the lack of the tyrosyl radical signal. First, the presence of a hydrogen-bonding network (see Scheme 2) could result in a loss of the characteristic absorption of tyrosyl radical. Second, the amine in the dpa arms functions as an electron donor instead of tyrosine. Previous electrochemical studies of similar complex[16] and a derivative of methylated tyrosine[24] showed that the hydrogen-bonded tyrosine had lower oxidation potential than the second non-hydrogen-bonded amine. Therefore, hydrogen-bonded tyrosine is a more feasible electron donor thermodynamically, but the involvement of amine could not be excluded at this stage. The conclusion of tyrosine being the electron donor is further supported by EPR measurements described below.

EPR Measurements. To further support our conclusion that the tyrosine functions as an electron donor, we studied the system by means of EPR that is sensitive for detecting radicals. For EPR measurements, the RuTP−TiO_2 sample prepared on a glass slip was scraped off and the resulting powder was mixed with acetonitrile. The colloidal solution obtained was deposited in a glass capillary (1 mm inner diameter) and then transferred to the resonant cavity. First the dark spectrum was recorded and then the spectrum under continuous light illumination. The spectrum recorded in the dark did not show any EPR signal. Illumination with continuous light in the cavity resulted in the appearance of a weak radical signal with peak-to-trough line width of approximately 16 G and $g = 2.0046$ (Figure 6). The signal disappeared within a few seconds after the initiating light was switched off, and the dark spectrum taken after illumination was similar to the spectrum recorded before illumination.

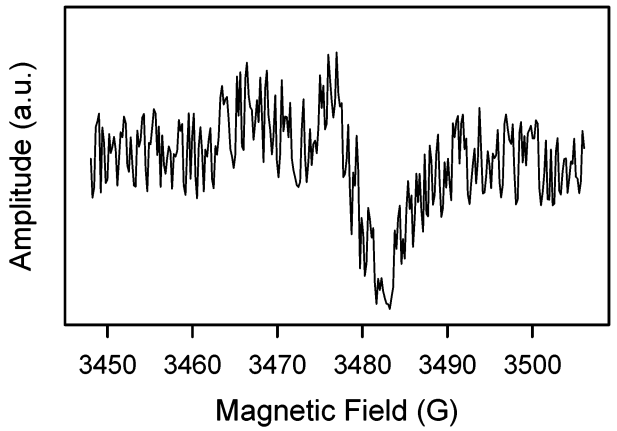

Figure 6. EPR spectrum recorded during illumination of RuTP−TiO_2 at room temperature. The spectrum is centered at $g = 2.0046$. The following EPR setting parameters were used: microwave power 50 mW, field modulation amplitude 3 G, time constant 20 ms.

Repeated light and dark cycles showed similar results: reversible formation of the signal in response to light and decay of the signal after a short dark interval. The last observation indicates the absence of light-induced damage of the sample during multiple illuminations.

The obtained *g* value and line width of the signal are typical for deprotonated phenoxyl radicals and show that a phenoxyl radical is the source of the photogenerated EPR signal.[16] We also investigated RuAla−TiO_2 by similar EPR measurements and did not find any light-induced signals. Therefore we conclude that tyrosine is the dominant electron donor in the intramolecular ET reaction in RuTP−TiO_2. On the basis of this conclusion, we propose that the lack of the characteristic absorption band of a tyrosine radical at 410 nm in the optical measurements is caused by hydrogen bonding that changes the spectroscopic properties of the tyrosine radical.

4. Mechanistic Considerations

From the results discussed above, we propose that the photoinduced multistep electron-transfer mechanism in the RuTP−TiO_2 system is as follows (Scheme 2): After light excitation of the ruthenium chromophore, electron injection occurs from its MLCT excited state to TiO_2, producing the charge-separated state of Ru(III) and electrons in the conduction band of TiO_2. The photogenerated Ru(III) is then reduced to Ru(II) by a fast (550 ns) intramolecular ET reaction from the hydrogen-bonded tyrosine with a quantum yield of 90%. It is worth noting that, in a similar ruthenium−tyrosine system without dpa arms,[14] the tyrosine can also serve as electron donor to Ru(III) but the quantum yield of intramolecular ET is only 15%. We propose that the reason for this is intramolecular hydrogen bonding between the phenolic hydroxyl group and the dpa arms in RuTP. This should facilitate the electron transfer reaction similarly to the situation present in natural photosynthesis.[25] When the tyrosine is unsubstituted, the intramolecular ET competes less efficiently with the charge recombination process, resulting in the low quantum yield.

5. Conclusions

Synthesis and characterization of a new supramolecular ruthenium complex partially mimicking the interactions of P_{680}, $tyrosine_Z$, and $histidine_{190}$ in photosystem II is described. After being attached onto the nanocrystalline TiO_2 film via ethyl carboxylate groups on the bipyridine ligands, light-induced ultrafast electron injection occurs from the MLCT state of RuTP to the conduction band of TiO_2. The resulting Ru(III) is reduced by intramolecular ET from the hydrogen-bonded tyrosine. The efficiency is as high as 90%, moving the positive holes away from the surface of TiO_2. Thus, besides mimicking the electron donor side of photosystem II, the RuTP−TiO_2 system is of interest for constructing dye-sensitized solar cell systems as well, since the fast and efficient removal of the hole from the surface prohibits back recombination. Another advantage of using tyrosine as electron donor is that the one-electron oxidation potential of tyrosine (0.84 V vs SCE)[16] is higher than that of triarylamine (0.65 V vs SCE)[3] and phenothiazine (0.72 V vs SCE).[12b] This should facilitate the hole transfer from the oxidized donor to the redox mediator in solution, a process crucial for the function of the regenerative dye-sensitized solar cells.[2]

Acknowledgment. We thank Dr. Torbjörn Pascher for technical assistance. This research is supported by grants from Delegationen för Energiförsörjning i Sydsverige, the Swedish Energy Agency, and the Swedish Research Council.

References and Notes

(1) O'Regan, B.; Grätzel, M. *Nature* **1991**, *353*, 737.

(2) (a) Grätzel, M. *Nature* **2001**, *414*, 338. (b) Hagfeldt, A.; Grätzel, M. *Chem. Rev.* **1995**, *95*, 49.

(3) Bonhote, P.; Moser, J.-E.; Humphry-Baker, R.; Vlachopoulos, N.; Zakeeruddin, S. M.; Walder, L.; Grätzel, M. *J. Am. Chem. Soc.* **1999**, *121*, 1324.

(4) (a) Heimer, T. A.; D'Arcangelis, S. T.; Farzad, F.; Stipkala, J. M.; Meyer, G. J. *Inorg. Chem.* **1996**, *35*, 5319. (b) Asbury, J. B.; Hao, E.; Wang, Y.; Lian, T. *J. Phys. Chem. B* **2000**, *104*, 11957.

(5) (a) Galoppini, E.; Guo, W.; Qu, P.; Meyer, G. J. *J. Am. Chem. Soc.* **2001**, *123*, 4342. (b) Galoppini, E.; Guo, W.; Zhang, W.; Hoertz, P. G.; Qu, P.; Meyer, G. J. *J. Am. Chem. Soc.* **2002**, *124*, 7801.

(6) Kleverlaan, C. J.; Indelli, M. T.; Bignozzi, C. A.; Pavanin, L.; Scandola, F.; Hasselman, G. M.; Meyer, G. J. *J. Am. Chem. Soc.* **2000**, *122*, 2840.

(7) (a) Benkö, G.; Kallioinen, J.; Korppi-Tommola, J. E. I.; Yartsev, A. P.; Sundström, V. *J. Am. Chem. Soc.* **2002**, *124*, 489 and references therein. (b) Benkö, G.; Myllyperkiö, P.; Pan, J.; Yartsev, A. P.; Sundström, V. *J. Am. Chem. Soc.* **2003**, *125*, 1118. (c) Piotrowiak, P.; Galoppini, E.; Wei, Q.; Meyer, G. J.; Wiewior, P. *J. Am. Chem. Soc.* **2003**, *125*, 5278.

(8) He, J.; Benkö, G.; Korodi, F.; Polivka, T.; Lomoth, R.; Åkermark, B.; Sun, L.; Hagfeldt, A.; Sundström, V. *J. Am. Chem. Soc.* **2002**, *124*, 4922.

(9) Pan, J.; Benkö, G.; Xu, Y.; Pascher, T.; Sun, L.; Sundström, V.; Polivka, T. *J. Am. Chem. Soc.* **2002**, *124*, 13949.

(10) (a) O'Regan, B.; Moser, J.; Anderson, M.; Grätzel, M. *J. Phys. Chem.* **1990**, *94*, 8720. (b) Haque, S. A.; Tachibana, Y.; Klug, D. R.; Durrant, J. R. *J. Phys. Chem. B* **1998**, *102*, 1745. (c) Kelly, C. A.; Farzad, F.; Thompson, D. W.; Stipkala, J. M.; Meyer, G. J. *Langmuir* **1999**, *15*, 7047.

(11) Kleverlaan, C.; Alebbi, M.; Argazzi, R.; Bignozzi, C. A.; Hasselman, G. M.; Meyer, G. J. *Inorg. Chem.* **2000**, *39*, 1342.

(12) (a) Argazzi, R.; Bignozzi, C. A.; Heimer, T. A.; Castelleno, F. N.; Meyer, G. J. *J. Am. Chem. Soc.* **1995**, *117*, 11815. (b) Argazzi, R.; Bignozzi, C. A.; Heimer, T. A.; Castelleno, F. N.; Meyer, G. J. *J. Phys. Chem. B* **1997**, *101*, 2591.

(13) Tommos, C.; Tang, X. S.; Warncke, K.; Hoganson, C. W.; Styring, S.; McCracken, J.; Diner, B. A.; Babcock, G. T. *J. Am. Chem. Soc.* **1995**, *117*, 10325 and references therein.

(14) Ghanem, R.; Xu, Y.; Pan, J.; Hoffmann, T.; Andersson, J.; Polivka, T.; Pascher, T.; Styring, S.; Sun, L.; Sundström, V. *Inorg. Chem.* **2002**, *41*, 6258.

(15) (a) Svensson, B.; Etchebest, C.; Tuffery, P.; van Kan, P.; Smith, J.; Styring, S. *Biochemistry* **1996**, *35*, 14486. (b) Hays, A.-M. A.; Vassiliev, I. R.; Golbeck, J. H.; Debus, R. J. *Biochemistry* **1998**, *37*, 11352. (c) Mamedov, F.; Sayre, R. T.; Styring, S. *Biochemistry* **1998**, *37*, 14245.

(16) Sun, L.; Burkitt, M.; Tamm, M.; Raymond, M. K.; Abrahamsson, M.; LeGourrierec, D.; Frapart, Y.; Magnuson, A.; Huang Kenez, P.; Brandt, P.; Tran, A.; Hammarström, L.; Styring, S.; Åkermark, B. *J. Am. Chem. Soc.* **1999**, *121*, 6834.

(17) Peek, B.M.; Ross, G. T.; Edwards, S. W.; Meyer, G. J.; Meyer, T. J.; Erickson, B. W. *Int. J. Pept. Protein Res.* **1991**, *38*, 114.
(18) Pascher, T. *Biochemistry* **2001**, *40*, 5812.
(19) (a) Juris, A.; Balzani, V.; Barigelletti, F.; Campagna, S.; Belser, P.; von Zelewsky, A. *Coord. Chem. Rev.* **1988**, *84*, 85 (b). Meyer, T. J. *Acc. Chem. Res.* **1989**, *22*, 163.
(20) Benkö, G.; Hilgendorff M.; Yartsev, A. P.; Sundström, V. *J. Phys. Chem. B* **2001**, *105*, 967.
(21) Magnusson, A.; Berglund, H.; Korall, P.; Hammarström, L.; Åkermark, B.; Styring, S.; Sun, L. *J. Am. Chem. Soc.* **1997**, *119*, 10720.
(22) Sjödin, M.; Styring, S.; Åkermark, B.; Sun, L.; Hammarström, L. *J. Am. Chem. Soc.* **2000**, *122*, 3932.
(23) Pan, J.; Lin W.; Wang, W.; Han, Z.; Lu, C.; Yao, S.; Lin, N.; Zhu, D. *Biophys. Chem.* **2001**, *89*, 193.
(24) Johansson, O.; Wolpher, H.; Borgström, M.; Hammarström, L.; Bergguist, J.; Sun, L.; Åkermark, B. *Chem. Commun.* **2003**, *2*, 194.
(25) (a) Tommos, C.; McCracken, J.; Styring, S.; Babcock, G. T. *J. Am. Chem. Soc.* **1998**, *120*, 10441. (b) Dorlet, P.; DiValentin, M.; Babcock, G. T.; McCracken, J. L. *J. Phys. Chem. B* **1998**, *102*, 8239. (c) Force, D. A.; Randall, D. W.; Britt, R. D. *Biochemistry* **1997**, *36*, 12062.